

# Functional anergy in a subpopulation of naive B cells from healthy humans that express autoreactive immunoglobulin receptors

J. Andrew Duty,<sup>1,3</sup> Peter Szodoray,<sup>1</sup> Nai-Ying Zheng,<sup>5</sup> Kristi A. Koelsch,<sup>1,4</sup> Qingzhao Zhang,<sup>1,4</sup> Mike Swiatkowski,<sup>5</sup> Melissa Mathias,<sup>1</sup> Lori Garman,<sup>1</sup> Christina Helms,<sup>1</sup> Britt Nakken,<sup>1</sup> Kenneth Smith,<sup>1</sup> A. Darise Farris,<sup>2,3,4</sup> and Patrick C. Wilson<sup>5,6</sup>

<sup>1</sup>Immunobiology and Cancer and <sup>2</sup>Arthritis and Immunology Research Program, Oklahoma Medical Research Foundation, Oklahoma City, OK 73104

<sup>3</sup>Department of Microbiology and Immunology and <sup>4</sup>Department of Pathology, The University of Oklahoma Health Sciences Center, Oklahoma City, OK 73104

<sup>5</sup>Section of Rheumatology, Department of Medicine and <sup>6</sup>Committee on Immunology, University of Chicago, Chicago, IL 60637

**Self-reactive B cells not controlled by receptor editing or clonal deletion may become anergic.** We report that fully mature human B cells negative for surface IgM and retaining only IgD are autoreactive and functionally attenuated (referred to as naive IgD<sup>+</sup>IgM<sup>-</sup> B cells [B<sub>ND</sub>]). These B<sub>ND</sub> cells typically make up 2.5% of B cells in the peripheral blood, have antibody variable region genes in germline (unmutated) configuration, and, by all current measures, are fully mature. Analysis of 95 recombinant antibodies expressed from the variable genes of single B<sub>ND</sub> cells demonstrated that they are predominantly autoreactive, binding to HEp-2 cell antigens and DNA. Upon B cell receptor cross-linkage, B<sub>ND</sub> cells have a reduced capacity to mobilize intracellular calcium or phosphorylate tyrosines, demonstrating that they are anergic. However, intense stimulation causes B<sub>ND</sub> cells to fully respond, suggesting that these cells could be the precursors of autoantibody secreting plasma cells in autoimmune diseases such as systemic lupus erythematosus or rheumatoid arthritis. This is the first identification of a distinct mature human B cell subset that is naturally autoreactive and controlled by the tolerizing mechanism of functional anergy.

## CORRESPONDENCE

Patrick C. Wilson:  
wilsonp@uchicago.edu

Abbreviations used: ANA, anti-nuclear antibody; BCR, B cell receptor; dsDNA, double-stranded DNA; HEL, hen egg lysozyme; MTG, MitoTracker Green; pTyr, phosphorylated tyrosine; SLE, systemic lupus erythematosus; ssDNA, single-stranded DNA; T3, transitional 3.

During B cell development, the near random nature of the VDJ recombination process leads to the unavoidable production of self-reactive antibodies. In fact, studies in humans have demonstrated that many if not most newly generated B cells are autoreactive (1). Extensive studies of self-tolerant B cells in transgenic mouse models have revealed the complicated systems of B cell selection used to avoid autoimmunity. Current models suggest that B cells expressing a transgenic surface Ig that binds DNA or protein autoantigens first attempt to alter the B cell receptor (BCR) by further variable gene rearrangement using “receptor editing” (2, 3). If receptor editing is unsuccessful, then the offending B cell may be eliminated by clonal deletion (4, 5) or it may enter maturity but with reduced or altered function so that it no longer

reacts to the self-antigens, which is referred to as clonal anergy (6–8). In this paper, we describe a human B cell population that is anergic. Clonal anergy was first conceived by Nossal and Pike in 1980 (6) to explain why injection of neonatal mice with high dosages of an antigen induced deletion of the specific B cells, whereas lesser dosages allowed retention of the specific B cells, but the cells were incapable of becoming antibody-secreting cells. In 1988, Goodnow et al. (8) demonstrated and characterized B cell anergy in vivo using the MD4/ML5 transgenic mouse model in which all B cells

© 2009 Duty et al. This article is distributed under the terms of an Attribution–Noncommercial–Share Alike–No Mirror Sites license for the first six months after the publication date (see <http://www.jem.org/misc/terms.shtml>). After six months it is available under a Creative Commons License (Attribution–Noncommercial–Share Alike 3.0 Unported license, as described at <http://creativecommons.org/licenses/by-nc-sa/3.0/>).

were self-specific to the neoself antigen hen egg lysozyme (HEL), and so cells surviving to maturity became anergic, having reduced surface BCR density, reduced proliferation and antibody secretion, and reduced  $\text{Ca}^{2+}$  flux and tyrosine phosphorylation responses (9–11).

The level and form of tolerance induction and the decision between anergic states or deletion is dependent on antigen form, specificity, and location of encounter. For example, soluble forms of the HEL (neoself) antigen allow survival of anti-HEL (autoreactive) but anergic B cells, whereas membrane-conjugated forms of HEL induce extensive deletion of HEL-specific B cells (12). It has recently been demonstrated that in the HEL model of anergy, the B cells are arrested at the immature transitional 3 (T3) stage of B cell development (13). In fact, it appears that all T3 B cells are naturally anergic even if the specificity is unknown (13, 14). Other levels of B cell functional inactivation or anergy vary depending on the particular autoantigen specificity of the transgenic mouse model (for review see reference 15). Antiinsulin B cells maintain normal levels of BCR signaling, such as calcium mobilization, but are attenuated for T cell-dependent responses, proliferation, and Ig production after toll-like receptor induction (16, 17). Anti-DNA B cells ( $V_H3H9$ ) that are specific for both double-stranded DNA (dsDNA;  $3H9 \times V_k4$ ) or single-stranded DNA (ssDNA;  $3H9 \times V_k8$ ) are each limited in their secretion of DNA-specific antibodies but vary for other functions. Although the ssDNA-reactive B cells have a relatively normal response to BCR cross-linking, the dsDNA-reactive B cells are unresponsive, they have limited proliferation responses, and they are blocked in development at the immature B cell stage (18–20). Intriguingly, a different anti-ssDNA transgenic mouse model (Ars/A1) is developmentally arrested at the T3 stage and has reduced BCR signaling, no proliferation, and no antibody secretion upon BCR cross-linking (13, 21). Transgenic B cells binding Smith (Sm) antigen are fairly normal but they only proliferate weakly and do not become fully mature plasma cells (22). Finally, in humans, B cells with natural autoreactivity for polyglutamine chains (the 9G4 idiotype) are excluded from normal B cell responses (23–25) and have attenuated BCR signaling capacity but appear to function normally in lupus patients (26). However, because natural autoreactivity is difficult to detect, little is known about the fate and phenotype of most autoreactive B cells in humans.

In this paper, we describe a population of naive-like human B cells that do not express IgM, only IgD ( $B_{ND}$  cells for short). Analysis of recombinant monoclonal antibodies demonstrated that most  $B_{ND}$  cells are autoreactive, binding antigens on human HEp-2 cells or DNA. The autoreactivity occurs naturally, as the cells have completely germline (unmutated) variable genes and are fully mature by all measures. We suspected that the autoreactive receptors of  $B_{ND}$  cells might lead to chronic stimulation and induction of anergy. Indeed, based on analysis of calcium flux and phosphorylated tyrosine (pTyr) levels after BCR cross-linkage,  $B_{ND}$  cells are functionally attenuated. Because  $B_{ND}$  cells can be fully activated by sufficient stimulation, we propose that these cells may be the

precursors that become high-affinity autoreactive B cells in diseases such as lupus or rheumatoid arthritis. The functional characterization of naturally autoreactive and anergic B cells herein is a critical step toward understanding and treating B cell mediated autoimmune pathology.

## RESULTS

### IgD<sup>+</sup>IgM<sup>-</sup> naive B cells from healthy humans express predominantly self-reactive BCRs

In transgenic mouse models of tolerance, B cells that predominantly express IgD isotype BCRs with low levels of surface IgM are anergic (9). We hypothesized that IgD<sup>+</sup>IgM<sup>-</sup>CD27<sup>-</sup> naive B cells of healthy humans (Fig. 1) might also be predominantly autoreactive and anergic. We therefore expressed recombinant monoclonal antibodies from isolated single B cells to test the specificity of naive B cell fractions (CD27<sup>-</sup>) that were IgD<sup>+</sup>IgM<sup>+</sup> (true naive) versus IgD<sup>+</sup>IgM<sup>-</sup>  $B_{ND}$  cells.  $B_{ND}$  cells made up 1–10% (typically  $2.5 \pm 0.716\%$ , SEM) of the naive B cells of 40 healthy adult blood donors (Fig. 1). Single B cells were sorted by flow cytometry into 96-well plates and amplified by multiplex single-cell RT-PCR to identify and clone the Ig heavy and light chain genes from a random assortment of B cells. To ensure that functional transcripts were cloned, RT-PCR primers were targeted to the variable gene leader sequences and to the respective constant region exons ( $C\mu$ ,  $C\delta$ ,  $C\kappa$ , or  $C\lambda$ ). The variable genes were then cloned into expression vectors and expressed with IgG and  $C\kappa$  or  $C\lambda$  constant regions in the 293A human cell line (1, 25, 27).

The production of antibodies that react to dsDNA are generally diagnostic of a pathological state in systemic lupus erythematosus (SLE) and other autoimmune diseases (28–30).  $B_{ND}$  cells produced anti-DNA reactivity nearly fourfold more

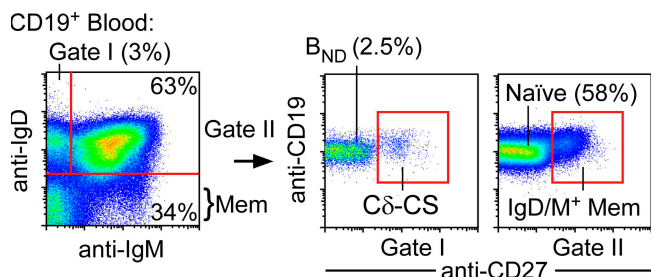


**Figure 1.**  $B_{ND}$  cells are gated as the IgD<sup>+</sup>IgM<sup>-</sup>CD27<sup>-</sup> cell fraction.

Peripheral blood B cells (CD19<sup>+</sup>) from humans are separated according to expression of IgM and IgD and then can be further distinguished by the CD27 expression that is found on memory B cells and plasma cells. On average, 3% of all B cells are found in the IgD-only fraction (gate I) where we find  $B_{ND}$  cells (2.5%), which can be further distinguished from another IgD-only population in blood, Cδ-CS cells (0.5%), by CD27 expression. Naive B cells, representing the bulk of peripheral blood B cells (58%), are found in the double-positive fraction (gate II) and can be further separated from IgD<sup>+</sup>, IgM<sup>+</sup>, memory, or marginal zone (MZ) cells by CD27 expression. The remaining fractions (IgM only and double negative) represent IgM memory and class-switched memory B cells, respectively, and are CD27<sup>+</sup>. All population percentages shown here represent the averages from analysis of 40 healthy adult blood donors.

frequently than naive B cells in a relative comparison. The frequency of anti-DNA antibodies produced from naive versus B<sub>ND</sub> cells was evaluated by ELISA. Antibodies were expressed from 87 naive B cells ( $n = 16, 37, 10, 10$ , and 14 by donor) and from 95 B<sub>ND</sub> cells ( $n = 17, 21, 30$ , and 27 by donor). For comparison, we also expressed the variable genes encoding

two well characterized antibodies that are used commonly to study anti-DNA reactivity (Fig. 2 A, red lines), including 3H9 (Fig. 2 A, squares) (2), and HN241 (Fig. 2 A, triangles) (29). Anti-DNA binding affinity was determined by regression analysis of the binding curves (see Materials and methods). The positive control antibody 3H9 was used to normalize all

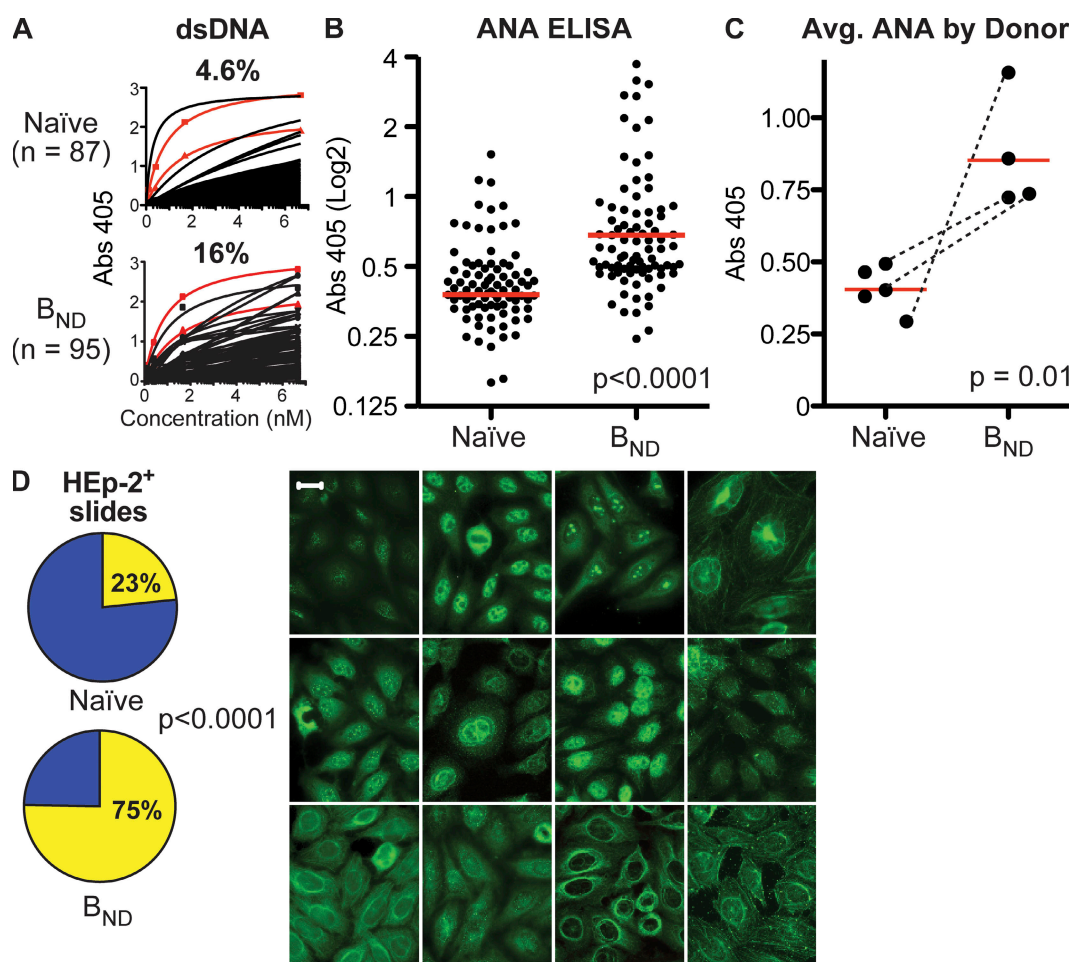


**Figure 2. B<sub>ND</sub> cells express autoreactive antibodies.** Recombinant monoclonal antibodies were expressed by transfection of human 293 cells with the variable genes from single B<sub>ND</sub> (totaling 95 clones;  $n = 17, 21, 30$ , and 27) or naive B cells (totaling 87 clones;  $n = 16, 37, 10, 10$ , and 14 by donor) and tested for binding to dsDNA and to antigens within the human HEp-2 cell line. (A) ELISA analysis to determine the frequency of B<sub>ND</sub> and naive B cells that bind to dsDNA. The variable genes encoding classical anti-DNA antibodies were also added (red lines), including 3H9 (squares) (2), and HN241 (triangles) (29). Both control antibodies were expressed as chimeric mouse/human IgG- $\kappa$  recombinant monoclonals identically to the naive and B<sub>ND</sub> antibodies so that all capture and detection reagents used were identical. Absorbencies were measured at OD<sub>415</sub> (y axis) and normalized to the 3H9-positive control antibody included on every plate. Binding to DNA is plotted for the various antibodies at 1  $\mu\text{g/ml}$  (6.67 nM) and three additional fourfold serial dilutions (x axis indicates nanomoles). Saturation curves were used to calculate relative affinities to determine if antibodies were positively reactive. (B) ELISA screens were performed to determine the amount of ANA reactivity. The B<sub>ND</sub> and naive monoclonal antibodies from A were loaded at a concentration of 25  $\mu\text{g/ml}$  onto commercially available ANA antigen ELISA plates. Absorbencies were measured at OD<sub>415</sub> and compared and normalized to an in house positive clone, C8-CS clone B09 (25). The absorbencies of naive versus B<sub>ND</sub> clones were significant by either Student's *t* test to compare means or Mann-Whitney to compare the medians ( $P < 0.0001$  for either test; median absorbencies are indicated as red lines). (C) Antibody absorbencies from B averaged and compared by donor for naive population and B<sub>ND</sub> population, including three matched comparisons of naive versus B<sub>ND</sub> antibodies indicated with dotted lines. The B<sub>ND</sub> cells were more often ANA reactive on average between donors ( $P < 0.02$  by Student's *t* test with Welch's correction for unequal variance and  $P = 0.016$  by Mann-Whitney test in comparing the medians). (D) HEp-2 reactivity was verified using immunofluorescence. Of the 95 antibodies derived from B<sub>ND</sub> cells, 72 (75%) were clearly reactive with human HEp-2 cells. 20/87 (23%) of the antibodies from naive cells were HEp-2 reactive. Representative antigen binding patterns on HEp-2 slides for antibodies from B<sub>ND</sub> cells are shown. Significance was established by  $\chi^2$  analysis;  $P < 0.0001$ . Commercial HEp-2 slides were stained with recombinant monoclonal antibodies and with antihuman IgG-FITC secondary antibody and visualized using fluorescence microscopy. Bar, 20  $\mu\text{m}$ .

ELISA plates. Antibodies with  $B_{MAX}$  absorbencies that were greater than the 95% confidence interval of the low positive control (HN241) and had measured affinities of  $>7$  nM (half-maximal binding at  $\sim 1$   $\mu$ g/ml) were scored as DNA binding. As indicated, of 95 antibodies from  $B_{ND}$  cells, 16% bound dsDNA, which is nearly fourfold more frequent than antibodies from the 87 naive cells, of which 4.4% bound dsDNA. The frequency of naive cells binding DNA was also similar to that reported previously by Wardemann et al. (1), whereas  $B_{ND}$  cells bound DNA at a frequency similar to that of early immature B cells before B cell selection. Analysis of insulin or LPS binding by ELISA found that although DNA-binding antibodies from naive cells are often polyreactive, only half of the  $B_{ND}$  cell-derived antibodies were polyreactive, and the remainder bound only DNA (Fig. S1, available at <http://www.jem.org/cgi/content/full/jem.20080611/DC1>).

Analysis of sera antibodies for binding to HEp-2 cells detected by indirect immunofluorescence is a classical test of autoreactivity. This antinuclear antibody (ANA) test is commonly used to assist with diagnosis of autoimmune diseases such as SLE (31). Three-quarters (72/95 or 75%) of the antibodies derived from  $B_{ND}$  cells were clearly reactive with human HEp-2 cells (Fig. 2 D, left). In contrast, consistent with previous reports (1, 25), only 23% (20 of 87) of the antibodies from naive cells bound to HEp-2 antigens ( $P < 0.0001$  by  $\chi^2$ ; Fig. 2 D, left). The HEp-2 binding patterns detected were quite variable, indicating a variety of autoreactivities, but, notably, the majority of  $B_{ND}$  cell antibodies bound to cytoplasmic antigens (Fig. 2 D, right). In addition, a quantitative assessment of the HEp-2 reactivity was determined using commercial ELISA-based ANA kits (Fig. 2 B). These assays demonstrated that ANA binding was significantly higher in the  $B_{ND}$  population compared with the naive cell antibodies both when mean or median binding is assessed for all antibodies ( $P < 0.0001$  for either Student's  $t$  test or Mann-Whitney test; Fig. 2 B) and when compared between donors ( $P < 0.02$  by Student's  $t$  test with Welch's correction for unequal variance and  $P = 0.016$  by Mann-Whitney test; Fig. 2 C). In conclusion, unlike  $IgM^+IgD^+$  naive B cells, most  $B_{ND}$  cells express autoreactive Igs.

### **$B_{ND}$ cells are mature naive-like B cells**

As immature B cells before completing primary selection may be autoreactive, we hypothesize that  $B_{ND}$  cells might be immature. However,  $B_{ND}$  cells do not express markers found on immature B cells such as the B cell progenitor marker CD10 and, like mature cells, express only low levels of the development markers CD38 and CD24, which are commonly used to distinguish recent BM immigrant immature/transitional B cells that are  $CD38^{hi}CD24^{hi}$  (Fig. 3 A) (32). Furthermore, the  $B_{ND}$  and naive populations are both positive for the BCR-associated regulator CD22 that is expressed on mature B cells (33). In addition, recent reports have demonstrated that transitional B cells, as well as  $CD27^+IgG^+$  memory cells, in circulation can be distinguished because they do not express the ATP binding cassette ABCB1 transporter and, subsequently, they retain mitochondrial dyes such as Rhodamine 123 or

MitoTracker Green (MTG) (34). Like naive cells,  $B_{ND}$  cells actively extrude MTG, further demonstrating that they are neither transitional B cells nor are they memory cells (Fig. 3 A, middle). Finally,  $B_{ND}$  cells do not produce CD179a (surrogate light chain; VpreB) transcripts, which distinguishes them from an autoreactive population of naive B cells that are in the process of receptor editing (35, 36) (Fig. 3 A, bottom).

Besides IgD expression,  $B_{ND}$  cells also express other molecules found only on mature circulating B cells including CD23, CD44, and CD40 (Fig. 3 B). Lack of CD38 also distinguishes  $B_{ND}$  cells from germinal center and plasma cells. Furthermore, like naive cells,  $B_{ND}$  cells are not proliferating ( $CD71^-$ ) and express neither the T cell costimulatory molecule CD80 nor the programmed cell death receptor CD95 (Fas), which are found on germinal center and memory B cells (Fig. 3 C). Finally, like naive cells, most  $B_{ND}$  cells express little CD5 protein (Fig. 3 B) but, interestingly, included some cells that were  $CD5^{low}$ , which is consistent with previous reports that CD5 expression is heterogeneous for various human B cell subsets (37). CD5 expression in mice marks the B1a subset of innate B cells and is known to be involved in negative regulation (38). The distinction of CD5 as a lineage marker is not established for human B cell populations, but it has been proposed to be a marker of activation (39). Although a connection of  $B_{ND}$  cells to a B1 cell type can't be completely ruled out, we conclude that in addition to autoreactive BCRs,  $B_{ND}$  cells are mature resting B cells that are most similar to naive B cells.

### **$B_{ND}$ cells are naturally autoreactive, having no evidence of previous immune experience**

Activated B cells rapidly proliferate and accumulate somatic mutations in the antibody variable genes to hone the specificity of the BCR. The cells also undergo class switch recombination to alter the antibody isotype. Variable regions from 228 gene sequences were analyzed from  $B_{ND}$  cells of nine blood donors and compared with historical data in the laboratory from various other B cell subpopulations (24, 25, 40–42).  $B_{ND}$  cells were analyzed from the four donors that antibodies were derived plus an additional five blood donors. As indicated in Fig. 4 A, there were no somatic mutations on the  $B_{ND}$  cell variable genes, indicating that the autoreactivity detected is natural and not generated during an immune response. In addition, no two  $B_{ND}$  cells sharing the same VDJ junctions were detected, likely indicating that they have not been clonally expanded. Finally, there is a small population of germinal center, memory, and plasma cells that have class switched to IgD at the genetic level (referred to as C $\delta$ -CS) and so are also  $IgD^+IgM^-$  (43, 44). These cells also express autoreactive IgD receptors (25). However, PCR analysis found no evidence of recombination junctions between the  $\mu$  and  $\delta$  switch regions for  $B_{ND}$  cells (Fig. 4 B), indicating that IgD is expressed as a splice product of VDJ-C $\mu$ -C $\delta$  transcripts and that  $B_{ND}$  cells have not undergone class switch recombination. C $\delta$ -CS B cells also have excessive somatic mutations of the variable genes and use predominantly Ig $\lambda$  light chains,



further distinguishing them from  $B_{ND}$  cells (Fig. 4 A). Interestingly, further indicating an autoreactive phenotype (1, 24, 35),  $B_{ND}$  cells use predominantly  $J_H6$  gene segments to encode antibodies (Fig. 4 C). In addition, variable genes from B cells of humans with lupus and in mouse models of lupus (mrl/lpr mice) tend to have long CDR segments (45–47). Cells with long CDR3s are also counterselected during normal human B cell development (1). As indicated in Fig. 4, both the frequency of  $B_{ND}$  cells with long CDR3 segments (Fig. 4 D) and the mean CDR3 length (Fig. 4 E) is significantly increased for  $B_{ND}$  cells. In conclusion,  $B_{ND}$  cells are naturally autoreactive with no evidence of ever having been involved in an immune response.

### $B_{ND}$ cells display reduced mobilization of intracellular calcium after BCR cross-linkage

In mouse models, self-reactive B cells that constitutively bind autoantigens become anergic, resulting in diminished downstream signaling events upon BCR cross-linkage (11, 48–50). We hypothesized that the  $B_{ND}$  cell population would also exhibit reduced signaling capacity upon activation because they are autoreactive. Immediately detectable measurements of BCR signaling that are reduced in anergic B cells of mice include the degree of intracellular calcium flux and an overall decreased level of pTyr. To avoid prematurely stimulating the B cells, thus depleting calcium stores and affecting pTyr levels, a negative enrichment scheme was used to isolate the

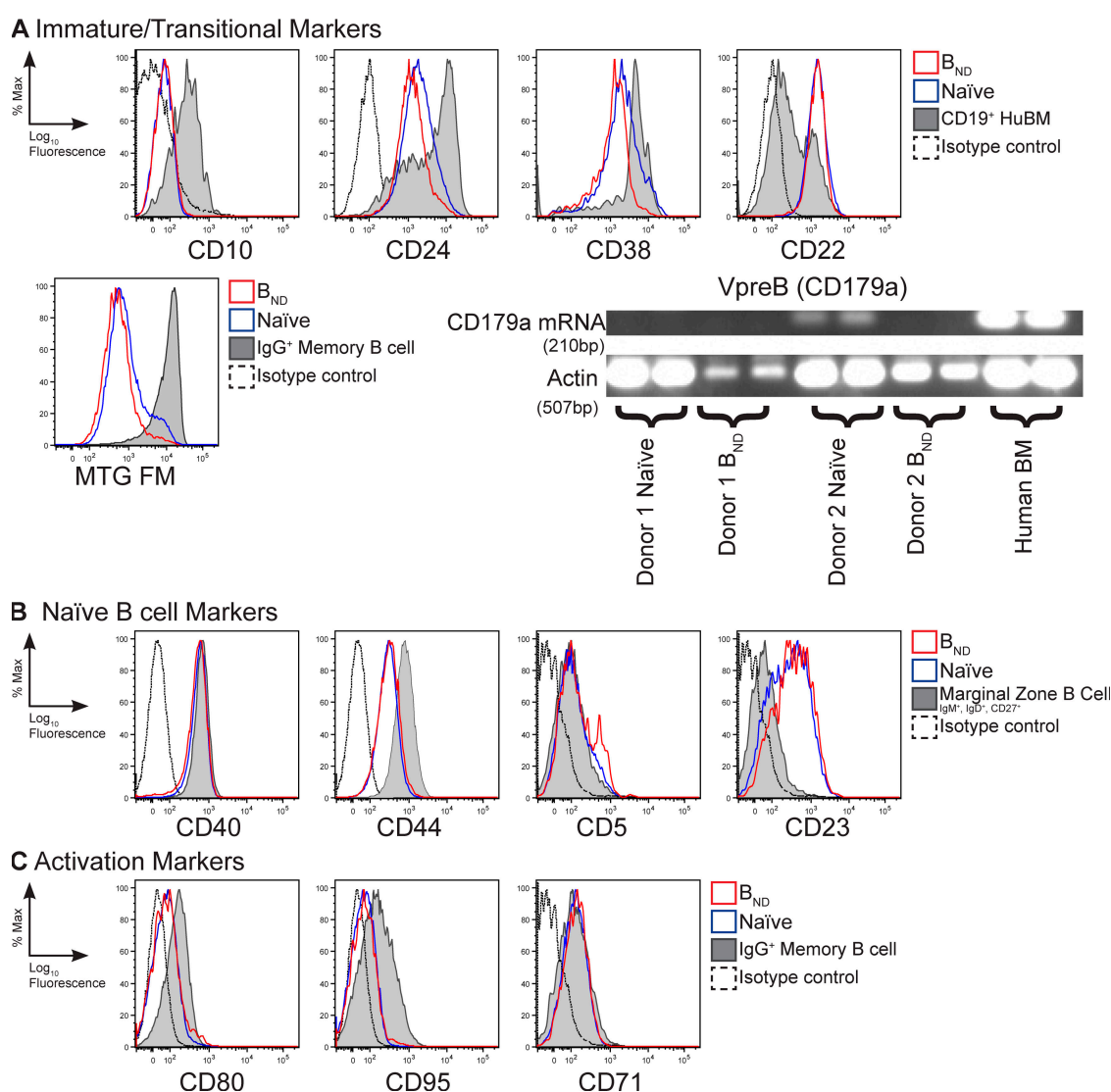


**Figure 3. The  $B_{ND}$  phenotype is naïve mature B cells.** Peripheral blood B cells were isolated and stained with anti-CD19, CD27, IgM, and IgD, as well as one of each of the antibodies shown in the figure, to delineate phenotype differences between  $B_{ND}$  and naïve populations for immaturity (A), maturity (B), or activation markers (C). Isotype controls were included and, where appropriate, CD19<sup>+</sup> human BM, marginal zone-like peripheral blood B cells (CD19<sup>+</sup>, CD27<sup>+</sup>, IgM<sup>+</sup>, and IgD<sup>+</sup>), or fractions representing IgG memory B cells (CD27<sup>+</sup>, IgM<sup>+</sup>, and IgD<sup>+</sup>) were included for an internal positive and negative control. Histograms are representative of three to eight donors in at least three independent experiments. RT-PCR analysis was performed on sorted  $B_{ND}$  and naïve cells for the presence of VpreB (CD179a) transcripts. Actin RT-PCR was included as a template control.

$B_{ND}$  and control B cell populations. In brief,  $B_{ND}$  and naive B cells were enriched by differentially staining peripheral blood  $CD27^-$  B cells loaded with the calcium dye Fluo-4 either in the presence or absence of anti-IgM so that we could identify  $B_{ND}$  or naive cells, respectively (Fig. 5 A and Materials and methods). Baseline intracellular calcium levels were established for 30 s, followed by treatment with various anti-BCR antibodies. Physiologically, antigen should bind all surface Ig regardless of isotype (i.e., IgD versus IgM). Therefore,

to most accurately mimic physiological stimulation with antigen, we first used combined anti-IgM plus anti-IgD cross-linkage to stimulate the B cells. Upon anti-IgD/IgM stimulation, the  $B_{ND}$  population showed a dramatically decreased ability to flux intracellular calcium compared with a substantial biphasic flux from the naive population (Fig. 5 B). In comparison, the  $B_{ND}$  population gave a result similar to  $CD27^+IgM/D/G^-$  B cell (class switched) memory population representing both IgA and IgE memory cells, which, as predicted, do not

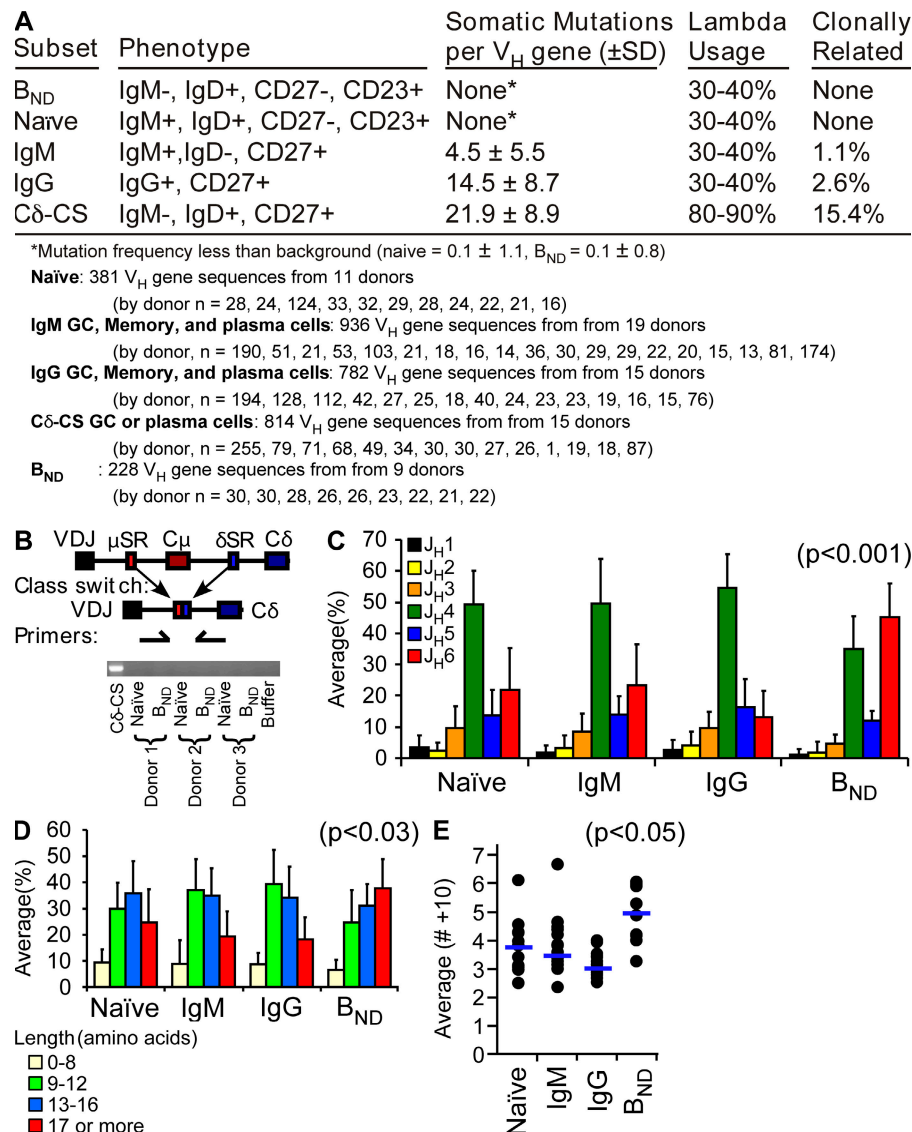


**Figure 4. The variable region sequences suggest that  $B_{ND}$  cells are most like naive cells.** (A) Sequence analysis from several healthy donors of  $B_{ND}$ , naive, IgG and IgM memory, and C $\delta$ -CS (C-delta class switch) revealed that  $B_{ND}$  cells, like naive cells, did not have somatic mutations in the variable region, are not clonally related as determined by common CDR3s, and use predominantly  $\kappa$  light chains. (B) PCR of genomic DNA for the constant chain switch regions between  $\mu$  and  $\delta$  revealed no DNA recombination at the delta locus and, thus, the  $B_{ND}$  cells are not class switched to DNA at the genomic level. (C) Comparison of heavy chain sequences for mean ( $\pm$ SD)  $J_H$  gene segment usage revealed increase use of  $J_H6$  (red bars) in  $B_{ND}$  cells compared with  $J_H6$  usage in naive, IgM, and IgG populations ( $P < 0.001$  by Student's  $t$  test between the  $B_{ND}$   $J_H6$  and separately  $J_H6$  in naive, IgM, and IgG populations;  $n$  values listed under the table in A). (D and E)  $B_{ND}$  cells had more amino acids on average ( $\pm$ SD) in their CDR3s as determined both by the frequency of cells with long CDR3s (17 aa<sup>+</sup>; red bars;  $P < 0.03$ ) and the mean CDR3 length for each donor (points) and averaged for all donors (blue bars) as compared with the other blood B cell populations (E;  $P < 0.05$ ; scale is amino acids  $>10$ ).

respond to anti-IgD/IgM stimulation. Representative kinetic graphs are shown for 25  $\mu\text{g}/\text{ml}$  of anti-IgM/D stimulant, representing three separate donors. Similar trends were also observed when various amounts of stimulant ranging from 10–50  $\mu\text{g}/\text{ml}$  were used, representing eight donors in three independent trials. On average, the peak mean fluorescence of Fluo-4 was significantly higher for naïve versus  $B_{\text{ND}}$ , which is indicative of a more robust flux of intracellular calcium

(Fig. 5 E;  $P < 0.05$  by Student's  $t$  test). Similarly, BCR cross-linking with anti- $\kappa/\lambda$  resulted in reduced  $B_{\text{ND}}$  calcium flux (Fig. S2 B, available at <http://www.jem.org/cgi/content/full/jem.20080611/DC1>). This difference was not caused by a variegated uptake of the calcium dye Fluo-4 or reduced viability because calcium peaks between the  $B_{\text{ND}}$  and naïve populations were equal when treated with the ionophore ionomycin (Fig. 5 D).

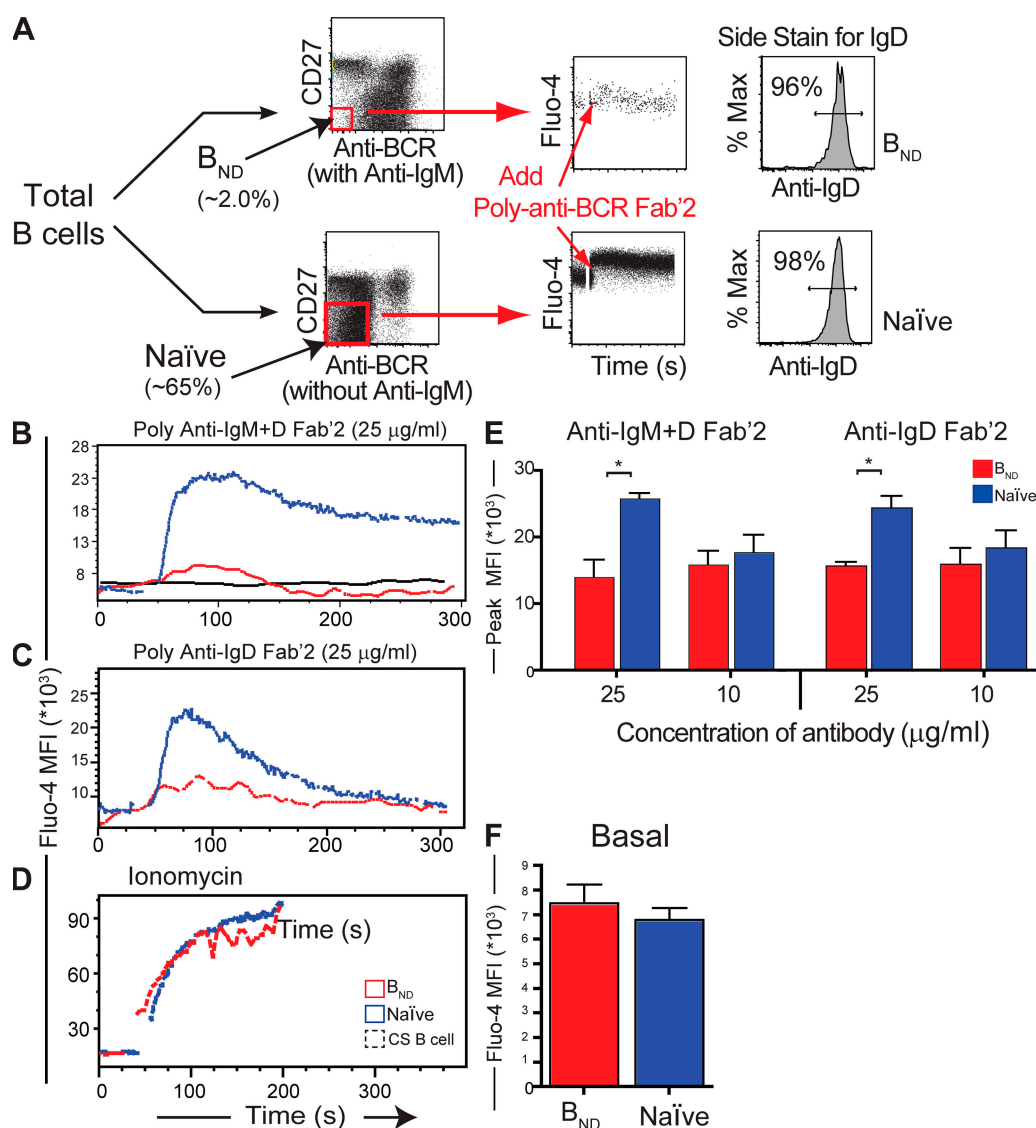


**Figure 5.  $B_{\text{ND}}$  cells have attenuated calcium responses compared with naïve cells after BCR cross-linking.** (A) A representative scheme of isolation and negative enrichment for the  $B_{\text{ND}}$  and naïve populations. Negatively enriched B cells from human peripheral blood were split into two equal fractions: one stained with anti-CD27, anti-IgM, and anti-IgG (anti-BCR) to negatively gate  $B_{\text{ND}}$  cells and the other with anti-CD27 and anti-IgG (anti-BCR) to negatively gate naïve cells. Cells were loaded with calcium dye Fluo-4 (Invitrogen) and transferred to flow cytometer, warmed to 37°C, and treated with different amounts and combinations of polyclonal Fab'2 BCR cross-linkers. Side stains were performed with these antibodies plus anti-CD19 and anti-IgD to test for population purity. In each case, B cell purities were >98% and  $B_{\text{ND}}$  and naïve purities were >96% as indicated. Calcium curves were determined using average mean fluorescence intensity (MFI) over time. (B) Representative kinetic graphs of average Fluo-4 MFI over time for naïve,  $B_{\text{ND}}$ , and a B cell class-switched memory control (CS B cell) population representing IgA/E<sup>+</sup> memory cells (CD27<sup>+</sup>, IgM<sup>+</sup>, IgG<sup>+</sup>, and IgD<sup>+</sup>; black line). Basal levels were established for 30 s and then the cells were treated with 50  $\mu\text{g}/\text{ml}$  of anti-IgM Fab'2/anti-IgD Fab'2, 50  $\mu\text{g}/\text{ml}$  of anti-IgD Fab'2 alone (C), or 20  $\mu\text{g}/\text{ml}$  ionomycin (D). (E) Maximal peak fluorescence of Fluo-4 was averaged  $\pm$ SD for B and C (\*,  $P < 0.05$ ;  $n = 3$  donors; Student's  $t$  test). (F) Mean fluorescence of Fluo-4  $\pm$ SD representing the basal levels (the first 30 s) was calculated showing a slightly higher amount in the  $B_{\text{ND}}$  population.

One possibility was that the reduced calcium response was because the B<sub>ND</sub> population expresses only surface IgD whereas naive cells also express IgM (Fig. 1), thus resulting in different frequencies of BCR cross-linkage or in qualitative differences in the signaling cascade. To gain functional insight, the cells were stimulated with anti-IgD alone. Anti-IgD alone also resulted in significantly less activation of the B<sub>ND</sub> than the naive population (Fig. 5, D and E;  $P < 0.05$  by Student's *t* test). This indicates that the reduced signaling capacity in the B<sub>ND</sub> population was caused by an intrinsic overall reduction in receptor mediated signaling.

As reported for anergic B cells in mice (48, 51; for review see reference 15), basal calcium levels for the B<sub>ND</sub> population were 10% higher on average than for naive cells, which is consistent with chronic stimulation by self-antigen (Fig. 5 F). We conclude from these experiments that B<sub>ND</sub> cells have intrinsically attenuated BCR-induced calcium flux and that this anergized phenotype likely results from chronic exposure to self-antigen in vivo.

#### B<sub>ND</sub> cells accumulate less pTyr when activated by BCR cross-linking

In addition to calcium flux, the signaling cascade seconds and minutes after BCR cross-linkage results in overall increases of cellular pTyr levels. Because relatively few B<sub>ND</sub> cells can be isolated at any one time from human peripheral blood, we chose to analyze pTyr levels by using flow cytometry or "Phos-Flow." This powerful technique allows the quantification of both the pTyr magnitude for each individual cell and the frequency of cells affected. With this assay, total activated B cells are rapidly fixed seconds after receptor cross-linkage and before any manipulation that might reduce detectable pTyr levels. The phenotypes and pTyr levels of individual cells can then be resolved retrospectively by using immunostaining and detection on a flow cytometer (Fig. 6 A). Each B cell population was fractionated and depleted of other cell types. Naive and B<sub>ND</sub> cells were first enriched through sorting with anti-CD27 and anti-IgM antibodies. Naive cells are predominantly in the total CD27<sup>+</sup> fraction, B<sub>ND</sub> cells are predominantly in the IgM<sup>+</sup>CD27<sup>+</sup> fraction, and untreated cells that will not be activated by anti-IgM/D treatment are predominantly in the CD27<sup>+</sup>IgD<sup>+</sup>IgM<sup>+</sup> fraction (determined separately to be mostly IgG, IgA, or IgE<sup>+</sup> B cells). By spiking the anti-IgM/IgD Fab'2 cross-linking mix with a fluorescently labeled (FITC) anti-IgD and then staining with intracellular anti-CD20 and anti-pTyr after stimulation, fixation, and permeabilization, we could gate and resolve each B cell population to high purity (Fig. 6 A, left). As indicated in the middle of Fig. 6 A, poststimulation pTyr levels were much greater in naive B cells than in B<sub>ND</sub> cells after treatment with a combination of polyclonal anti-IgD/IgM for an optimal 45 s (determined separately to be the peak of activation; Fig. S2 A). The reduced pTyr induction is not caused by increased cell death or lack of viability in the B<sub>ND</sub> population, as both they and naive cells are stimulated to the same level with the phosphatase inhibitor pervanadate (orthovanadate H<sub>2</sub>O<sub>2</sub>; Fig. 6 A, right histogram).

On average, from multiple blood samples, B<sub>ND</sub> cells accumulated significantly less total tyrosine phosphorylation than naive cells at various anti-IgD/IgM concentrations (Fig. 6 B; significance for 10 and 50  $\mu$ g/ml is  $P < 0.05$  and 0.01, respectively by Student's *t* test). Each point in Fig. 6 B represents the mean and SD for at least three independent analyses of B<sub>ND</sub> or naive cells pooled from at least three different donors for each repetition. As with calcium, treatment with anti-IgD alone also caused greater reduction in pTyr induction in B<sub>ND</sub> cells than in naive B cells for each of three trials (Fig. 6 C). The red, green, and blue lines represent the cells from independent blood donors simultaneously assayed for anti-IgD alone (Fig. 6 C, left) or in combination with anti-IgM (Fig. 6 C, right). More specifically, Src family tyrosine kinases (Lyn, Fyn, and Blk), which are known to be important for transducing signals directly associated with receptor cross-linking, were evaluated for activation through detection of pTyr residue 416. Using calibration beads to establish absolute units, we found that in comparison to naive cells the B<sub>ND</sub> population had reduced pSrc levels upon treatment with anti-IgD and anti-IgM (Fig. 6 D;  $P < 0.05$  by Student's *t* test, based on three independent trials). In summary, pTyr levels were reduced for B<sub>ND</sub> cells after cross-linking in every instance for 12 independent trials (totaling 30 pooled blood donors). Interestingly, if B<sub>ND</sub> cells were rested overnight in culture, they phosphorylated tyrosines and fluxed calcium at similar levels as naive cells (Fig. S3 E, available at <http://www.jem.org/cgi/content/full/jem.20080611/DC1>), which is consistent with observations in transgenic mice where removal of the chronic self-stimulation rapidly allows return to a nonanergic state (52).

In conclusion, likely because of chronic self-stimulation, B<sub>ND</sub> cells are anergic, displaying reduced activation levels after BCR cross-linkage. This analysis suggests that B<sub>ND</sub> cells have a decreased ability to respond to antigen binding, thus avoiding the eventual secretion of autoantibodies. Future characterization of the specific signaling pathways disrupted in B<sub>ND</sub> cells should provide insight into the intrinsic mechanisms of immune tolerance for B cells and may identify specific pathways that can be therapeutically targeted to treat autoimmune diseases.

#### DISCUSSION

Mature and naive autoreactive (and thus potentially pathogenic) B cells in the periphery have been shown to account for up to 20% of the circulating B cell pool in healthy human adults (1, 25). The presence of these autoreactive cells begs many but ultimately two important questions: why have they survived selection and how are they tolerized? Focusing on the latter, extensive studies of self-tolerant B cells in transgenic mouse models over the last two decades have revealed the complicated systems of B cell selection used to avoid autoimmunity. B cells expressing transgenic surface Ig that bind DNA or protein autoantigens that do not alter the BCR by receptor editing (2, 3) may be eliminated (clonal deletion) (4). Importantly, and pertinent to this work, many autoreactive cells pass these checkpoints for reasons not well understood and survive



to the periphery, but with reduced or altered function so they no longer react to the self-antigens (clonal anergy) (7, 8).

A key advance to understanding and treating human autoimmune disease is to link the numerous fundamental dis-

coveries of the past 20 yr concerning autoreactive B cells in transgenic mice to immune tolerance in humans. Through analyses of a mature naive human B cell population, we have shown that, similar to the classical anti-HEL/HEL model of

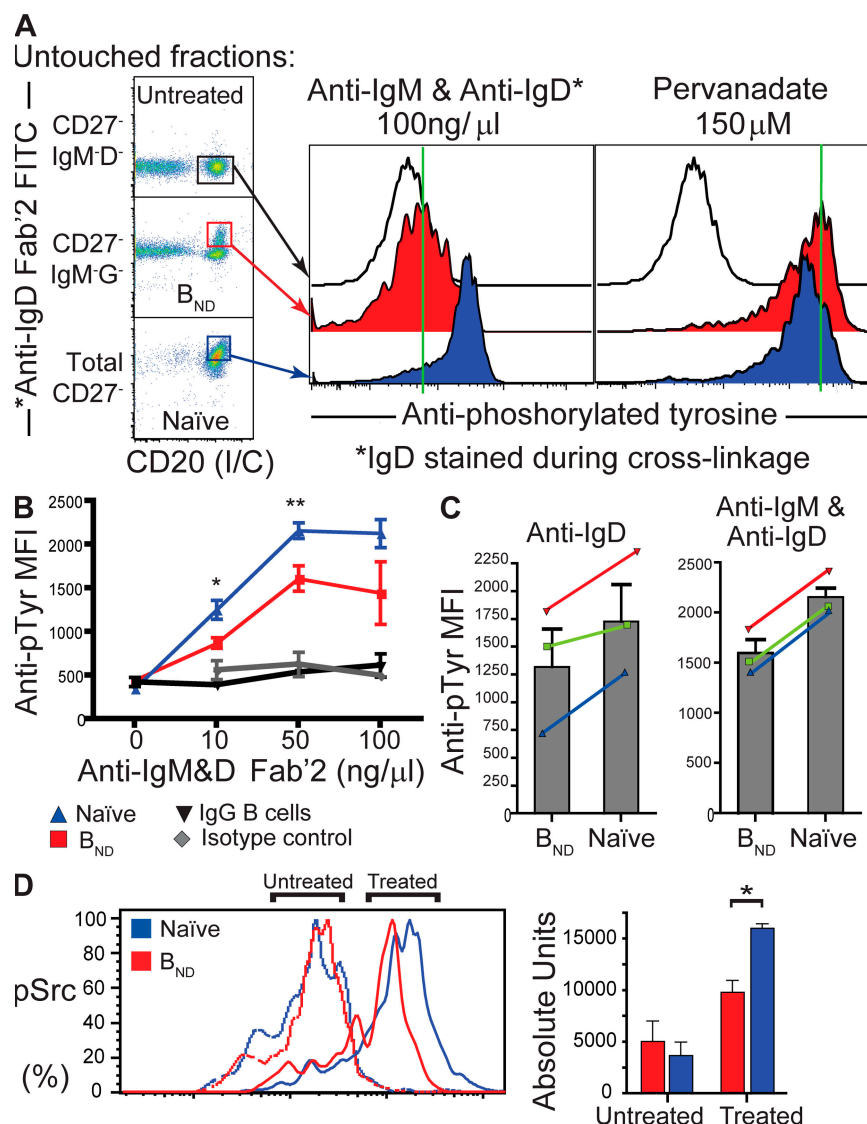


**Figure 6. B<sub>ND</sub> cells have reduced tyrosine phosphorylation, suggesting that they are natural anergic B cells.** (A) Representative histogram of treated B<sub>ND</sub> and naive cells sorted according to a least-touch strategy (see Materials and methods). 10<sup>5</sup> cells were incubated with anti-IgD Fab'2-FITC + IgM Fab'2 for 45 s at various concentrations, fixed, and permeabilized, followed by staining by anti-pTyr and intracellular anti-CD20. Histograms were built by FACS analysis and treated populations were compared with untreated controls. Cells were also stimulated with pervanadate as a positive control (right histogram). Green lines are used as qualitative references to mark the median fluorescence of the untreated controls, allowing a visual comparison of fluorescence shift with treated samples. (B) Cells were stimulated with anti-IgD Fab'2 FITC + IgM Fab'2 at concentrations of 10, 50, and 100 μg/ml to determine concentration dependency and were plotted as mean fluorescence intensity (MFI) ± SD of pTyr-PE (for each concentration point, *n* = 3 groups of 1–3 donors; \*, *P* < 0.05 and \*\*, *P* < 0.01 for 10 and 50 μg/ml, respectively, by Student's *t* test). Class switched B cells could also be gated (IgD<sup>+</sup>, IgM<sup>+</sup>, and CD20<sup>+</sup>; black line) from the peripheral set and are included as an internal negative control. Isotype controls (gray line) were established for the stimulated fractions. (C) Incubation of B<sub>ND</sub> and naive cells with 50 μg/ml of anti-IgD Fab'2 alone or in combination with anti-IgM. Results of three donors are plotted as MFI of pTyr. Error bars represent the mean ± SD. Color lines represent individual donor variation between naive and B<sub>ND</sub> population. (D) Cells were sorted as in A but stained with antiphosphorylated Src (pTyr 416; pSrc). Representative histograms are shown for naive and B<sub>ND</sub> cells, untreated and treated with anti-IgD Fab'2 FITC + anti-IgM Fab'2. Bar graphs represent the mean absolute number of units/molecules ± SD of phosphorylated Src as determined by Sphero Rainbow Calibration beads (Invitrogen) from three healthy donors and compared between B<sub>ND</sub> (red) and naive (blue) populations for both treated and untreated fractions. Significance for treated fractions (*P* < 0.05) was established by a Student's *t* test.

anergy developed by Goodnow (8), IgD<sup>+</sup> B cells with no surface IgM are predominantly autoreactive and are functionally attenuated. The mechanistic connection between anergy and reduced IgM expression is not known and is not a universal phenotype of all anergic B cells (for review see reference 15) but may represent a consequence of constant self-antigen exposure in the early life of the cell (53).

As described, anergy in the B<sub>ND</sub> population is not solely dependent on receptor density (or lack of surface IgM expression), as signaling through IgD alone was also less effective for B<sub>ND</sub> than for naive cells (Fig. 5 & 6). However, it is notable that naive cells responded differently to cross-linking by IgM versus IgD, suggesting that down-regulation of surface IgM could have functional consequences for the B<sub>ND</sub> cells. Though the initial burst of stimulation was similar with either cross-linking reagent, a subsequent plateau of sustained increased calcium levels was maintained after IgM stimulation but was lost after IgD stimulation (Fig. S2 C). Combined stimulation through both IgM and IgD resulted in an additive response, with an initial burst similar to either reagent alone, followed by a plateau of sustained calcium levels similar to the anti-IgM response. Thus, assuming that the anti-IgD and anti-IgM reagents similarly cross-link their respective target epitopes, the maintenance of anergy in B<sub>ND</sub> cells may also be influenced by the lack of surface IgM. The exact mechanism behind the receptor-mediated lack of response in the B<sub>ND</sub> population will need to be further elucidated.

B<sub>ND</sub> cells exhibit a well-characterized naive phenotype in that they are CD44<sup>+</sup>, CD23<sup>+</sup>, CD38<sup>-</sup>, CD95<sup>-</sup>, CD80<sup>-</sup>, and CD5<sup>-</sup>. They were not clonally expanded and had no somatic mutations. Importantly, B<sub>ND</sub> cells can also be distinguished from immature new BM immigrant B cells described in recent reports (1, 32) because the immature cells are CD44<sup>-</sup> and CD38<sup>+</sup> as well as being IgD<sup>-</sup> and IgM<sup>+</sup>. B<sub>ND</sub> cells also do not express surrogate light chains (CD179a), distinguishing them from preB cells, editing B cells, or recent bone emigrants from the BM (35, 36). Thus, B<sub>ND</sub> cells appear mature by all measures; however, we cannot rule out the possibility that they have recently transitioned from an immature state. Similarly, although the attenuated signaling of B<sub>ND</sub> cells demonstrated that these cells are anergic, we cannot completely rule out some specialized B cell differentiation similar to B1 or MZ cells in mice because these populations have not been well established in humans. However, based on all analyses to date we propose that B<sub>ND</sub> cells arise from autoreactive naive cells that have matured in the classical B-2 pathway.

Similarly to previous reports of anergy, B<sub>ND</sub> cells show attenuation in Ca<sup>2+</sup> response and a decrease in accumulation of phosphotyrosines upon treatment with BCR cross-linkers. However, much like anergic B cells in mice, an active mechanism and exposure to autoantigen appears necessary to maintain anergy because rest in tissue culture media overnight restores B<sub>ND</sub> cell signaling to levels similar to naive cells (Fig. S3). In addition, the function of B<sub>ND</sub> cells can be rescued when treated with the soluble T cell factors IL-4 and CD40L, leading them to proliferate, express CD80 and the proliferation

marker CD71, and differentiate into plasmablast-like CD-38<sup>hi</sup>CD27<sup>hi</sup> cells (Fig. S3). Thus, as in previous reports (52, 54, 55), anergy in the B<sub>ND</sub> population appears transient and reversible if the cells receive appropriate pro-T/B cell signals or if the cells are removed from the autoreactive environment. Importantly, Chang et al. (56) recently found that IgD<sup>+</sup>IgM<sup>low</sup>CD27<sup>-</sup> B cells that we suspect are B<sub>ND</sub> cells become increased in SLE patients. Unlike healthy people, in SLE patients these cells also displayed evidence of activation such as up-regulated CD80/86 levels. Thus, B<sub>ND</sub> cells may pose a serious danger in the development of acute or chronic autoimmune pathology, especially if T cell tolerance is also breached allowing helper activation of these autoreactive cells. We propose that the B<sub>ND</sub> population may be an important source of precursors for pathological autoantibody-secreting cells activated in lupus or other autoimmune diseases.

In conclusion, we have characterized a population of naturally autoreactive B cells in humans that have become anergic. We can now study the molecular and functional characteristics of this manifestation of anergy and its role in avoiding autoimmunity, or if these cells are not properly controlled, in causing autoimmune disease. Further, studies to elucidate the mechanisms inducing anergy may identify molecular pathways that can be exploited pharmacologically to induce an anergic state in reactive B cells to treat autoimmune diseases or avoid organ rejection.

## MATERIALS AND METHODS

**B cell enrichment, sorting, and FACS analyses.** B lymphocytes were isolated from the buffy coat component from 500 ml of freshly donated peripheral human blood obtained from the Oklahoma Blood Institute (Oklahoma City, OK) according to established National Institutes of Health guidelines and protocols with approval from the Oklahoma Medical Research Foundation Institutional Review Board. Lymphocytes were isolated by placement over a Ficoll density gradient to remove RBCs and other leukocytes followed by B cell-specific enrichment by negative magnetic bead selection as described previously (24, 40, 57). Cell sorting was performed by staining the cells with monoclonal antihuman antibodies against CD27-FITC, CD19-PE-Alexa Fluor 610 (Invitrogen), IgM-APC (SouthernBio-tech), and IgD-PE (BD). B<sub>ND</sub> and naive B cell populations were resolved as in Fig. 1 using a MoFlo flow cytometer (Dako) in the Oklahoma Medical Research Foundation flow core facility. For phenotype profiles, populations were resolved as in Fig. 1 and stained with various antihuman antibodies labeled with either FITC or PE fluorophores (Invitrogen), including monoclonal antibodies against CD38, CD44, CD80, CD71, CD95, CD138, CD5, CD179a, CD23, CD21, and Annexin-V. For analyses of mitochondrial dye retention, MTG FM dye (Invitrogen) was loaded into sorted B<sub>ND</sub> and naive B cell populations at a concentration of 100 nM for 30 min and chased with fresh media as previously described (34). For single-cell PCR, bulk cells of either phenotype were first sorted and then resorted into 96-well PCR plates to ensure purity of single cells (98–99% pure). FACS analysis was performed using flow core facility FACSCalibur, FACS Aria, or LSR-II flow cytometers (BD) and software analysis was performed with FlowJo Cytometric software (Tree Star, Inc.).

**Sequencing and repertoire analysis.** Cells were sorted into the different populations as indicated above and as previously described (24, 40, 57). V region amplification and sequence analysis was performed as described but, in brief, VH4 and VH3 family specific leader sense primers were paired with antisense primers to particular constant region gene ( $\mu$  or  $\delta$ ). These primers

included the following: VH4 sense primer, 5'-ATGAAACACCTGTG-GTTCTT-3'; C $\mu$  antisense primer, 5'-CACGTTCTTTTCTTTGTTC-3'; and C $\delta$  antisense primer, 5'-GTGTCTGCACCTGATATGATGG-3'. PCR products were amplified using TA or TOPO-TA cloning kits (Invitrogen), and plasmid purification was performed using the miniprep kit (QIAGEN). Sequencing was done at the Oklahoma Medical Research Foundation sequencing core. All V regions were analyzed using in house analysis software and the National Center for Biotechnology Information IgBlast server (<http://www.ncbi.nlm.nih.gov/igblast/>) or the Immunogenetics server ([http://imgt.org/IMGT\\_vquest/share/textes/](http://imgt.org/IMGT_vquest/share/textes/)).

For VpreB (CD179a) analysis, RNA was extracted from  $10^4$ – $10^5$  freshly sorted B<sub>ND</sub> and naive fractions using RNAWiz (Ambion), followed by One-Step RT-PCR (QIAGEN) RNA to cDNA amplification in 40 repeated cycles of equal RNA amounts, using the following primer sets: VpreB sense, 5'-GAGTCAGAGCTCTGCATGTCTG-3'; VpreB antisense, 5'-GTGAGGCCGATTGTGTTTCCAAG-3'; actin sense, 5'-TACCACTGGCATCGTGATGGACT-3'; and actin antisense, 5'-TCCTTCTGCATCCTGTGCGCAAT-3'. Direct PCR products were analyzed on 1% agarose gels with TAE buffer.

**Production of recombinant monoclonal antibodies from single human B cell.** In order to test the specificity of B<sub>ND</sub> cells, recombinant monoclonal antibodies were produced from the variable region genes of isolated single cells. Using a modified strategy similar to previous reports (1, 25, 36), single B cells were sorted by flow cytometry into 96-well plates, and the variable genes amplified by multiplex single-cell RT-PCR to identify and clone the Ig heavy and light chain genes from a random assortment of cells. These variable genes were then cloned into expression vectors and expressed with IgG constant regions in the 293A human cell line. A total of 95 antibodies from B<sub>ND</sub> cells ( $n = 17, 21, 30$ , and  $27$  by donor) were compared with 87 antibodies from naive B cells (IgD<sup>+</sup>IgM<sup>+</sup>CD38<sup>-</sup>;  $n = 16, 37, 10, 10$ , and  $14$  by donor). Three sets of naive and B<sub>ND</sub> antibodies were matched from individual donors. Each antibody was purified from the serum-free tissue culture media.

**ELISA and HEP-2 analyses for autoreactivity.** To screen the expressed antibodies for DNA reactivity or polyreactivity, ELISA microtiter plates (Costar; Corning) were coated with  $10 \mu\text{g/ml}$  of calf thymus ssDNA or dsDNA (Invitrogen), LPS (Sigma-Aldrich), or recombinant human insulin (Fitzgerald). Goat anti-human IgG ( $\gamma$  chain specific) peroxidase conjugate (Jackson ImmunoResearch Laboratories) was used to detect binding of the recombinant antibodies followed by development with horseradish peroxidase substrate (Bio-Rad Laboratories). Absorbencies were measured at OD<sub>415</sub> on a microplate reader (MDS Analytical Technologies). Antibody affinities to the various antigens were compared by endpoint regression analyses to predict the absorbencies expected based on the binding curve for four four-fold dilutions of antibody (beginning at  $1 \mu\text{g/ml}$ ,  $7 \text{ nM}$ ) against a fixed concentration of antigen. Antibodies with B<sub>MAX</sub> absorbencies that were above the 95% confidence interval of the low positive control (HN241) and had measured affinities of  $<7 \text{ nM}$  (half-maximal binding at  $\sim 1 \mu\text{g/ml}$ ) were scored as DNA binding. All antibodies were screened for ANA reactivity using the QUANTA Lite ANA ELISA kit (INOVA Diagnostics, Inc.) as per the manufacturer's direction. ANA results were verified on a subset of antibodies by immunofluorescence using commercial HEP-2 slides (Bion Enterprises) as previously described (1, 36) and as per the manufacturer's suggested protocol. HEP-2 slides were analyzed using a fluorescent microscope (Axio-plan II; Carl Zeiss, Inc.). All HEP-2 and ANA reactivity were compared with positive control sera from a lupus patient and to nonreactive sera from a healthy blood donor.

**Calcium flux.** Fresh human PBMCs from buffy coats were enriched for B cells (see B cell enrichment, sorting, and FACS analysis) and split into four equal fractions of  $10^6$  cells for each donor (1): naive (2), B<sub>ND</sub> (3), ionomycin naive (4), and ionomycin B<sub>ND</sub>. Cells were resuspended in preprepared HBSS containing  $1 \mu\text{M}$  Ca<sup>2+</sup> and  $1 \mu\text{M}$  Mg<sup>2+</sup> ions supplemented with 1% BSA and

were warmed to  $30^\circ\text{C}$  for 10 min. After temperature equilibration, cells were loaded with Fluo-4 AM calcium indicator (Invitrogen) at a final concentration of  $5 \mu\text{M}$  and incubated for 15 min in the dark. Cells were then washed and resuspended in HBSS/BSA containing  $2.5 \mu\text{M}$  Probenecid (Sigma-Aldrich) for an additional 30 min at  $30^\circ\text{C}$ . After calcium dye loading, cells were placed on ice and differentially stained for 30 min. The naive fractions, including ionomycin naive, received anti-CD27 PE (Invitrogen) and anti-IgG-APC (BD) antibodies. The B<sub>ND</sub> fractions, including ionomycin B<sub>ND</sub>, received anti-CD27 PE, anti-IgM-APC, and anti-IgG-APC. Cells were also stained with anti-CD3-Bio and streptavidin-PE (Invitrogen) to gate out T cells and other non-B cells that escaped column purification. Non-Fluo-4-loaded B cells from each donor were also simultaneously stained, but with the addition of anti-IgD to evaluate the purity of measured fractions. After staining, cells were washed in HBSS/BSA/Probenecid and placed at  $37^\circ\text{C}$  for 10 min. Cells were then placed on a LSRII flow cytometer and gates were drawn for the subpopulations naive and B<sub>ND</sub>. Baselines were read for 30 s, after which the cells were removed and stimulated with indicated amounts of Fab'2 anti-IgM (Jackson ImmunoResearch Laboratories) and Fab'2 anti-IgD (SouthernBiotech) or Fab'2 anti-IgD alone or Fab'2 anti- $\kappa/\lambda$  (SouthernBiotech) antibodies. Calcium curves were read for 5–7 min. In the ionomycin fractions,  $5 \mu\text{l}$  of  $1 \text{ mg/ml}$  ionomycin/EtOH (Sigma-Aldrich) was added 30 s after baseline reads to control for dye loading and cell activation potential. Kinetic curves for each calcium response were generated using FlowJo software.

**PhosFlow analysis.** Human B cells from blood buffy coats were isolated (see B cell enrichment, sorting, and FACS analysis) and split into two pools for sorting, one (pool 1) stained with anti-CD27-FITC and the other (pool 2) with anti-CD27-FITC and anti-IgM-APC. Pool 1 B cells were sorted for CD27-negative cells and represented primarily naive cells. Pool 2 cells, representing the B<sub>ND</sub> cells, were sorted for the IgM<sup>-</sup>CD27<sup>-</sup> population. Each pool was then washed and resuspended in RPMI without FCS and preheated to  $37^\circ\text{C}$ . The cells were then split into aliquots ( $10^5$  cells/tube) and incubated for 45 s with polyclonal anti-IgD Fab 2'-FITC (SouthernBiotech) and polyclonal anti-IgM Fab 2' (Jackson ImmunoResearch Laboratories). Cells were then immediately fixed with PhosFlow Fix Buffer I (BD) for 10 min at  $37^\circ\text{C}$ . Cells were then washed two times in PhosFlow Perm/Wash Buffer I (BD), and stained with anti-pTyr-PE (clone PY20; BD) or antiphosphorylated Src (phosphorylated Tyr 416; Cell Signaling Technology). Cells were simultaneously stained with intracellular anti-CD20-PerCP-Cy5.5 (clone H1-FB1; BD) at the amounts suggested by the manufacturer. For the pSrc analysis, Sphero Rainbow Beads (BD) were used at the amounts suggested by the manufacturer to calibrate the FACS machine for direct comparisons from multiple experiments. For a positive control, a separate fraction ( $10^5$ ) of each population was incubated for 5 min with  $5 \mu\text{l}$  of the protein tyrosine phosphatase inhibitor pervanadate/H<sub>2</sub>O<sub>2</sub> (3%  $100 \text{ mM}$  orthovanadate and 3% H<sub>2</sub>O<sub>2</sub> in dH<sub>2</sub>O). Populations were resolved using FACS and compared with an untreated control. All computational analysis was performed with FlowJo software.

**Statistical analyses.** Graphing and statistical analysis were performed using Prism software (GraphPad Software, Inc.) or Excel (Microsoft). For comparisons of antibody autoreactivity between total naive and B<sub>ND</sub> antibodies the  $\chi^2$  statistic was used. To compare the ANA values generated by the ANA ELISA assays, we used both Student's  $t$  tests to compare the means and Mann-Whitney tests to compare the medians. The Student's  $t$  tests were done with a Welch's correction because of unequal variances between the naive and B<sub>ND</sub> datasets (determined by the F test). However, although not significantly so, there was a non-Gaussian distribution notable in these datasets and, therefore, we also used the nonparametric Mann-Whitney test to compare the median distributions. Also, because of the non-Gaussian distribution the medians are noted in Fig. 2 rather than the means. PhosFlow analyses of pTyr levels and variable gene repertoire analyses used two-tailed Student's  $t$  tests (paired for PhosFlow analyses and heteroscedastic for the repertoire analyses).

**Online supplemental material.** Fig. S1 illustrates the frequency of poly-reactive antibodies PCR-cloned from the naive and B<sub>ND</sub> cells. Fig. S2 includes graphs of the time course of activation of naive versus B<sub>ND</sub> cells as measured by pTyr accumulation (A), calcium flux induced by anti- $\kappa$  light chain treatment (B), and an illustration of the qualitative differences in calcium flux comparing cross-linking of naive B cells through the IgM or IgD receptors individually and in combination (C). Fig. S3 illustrates the rescue of a functional state for B<sub>ND</sub> cells by stimulation with cofactors such as CD40L, IL-4, and IL-10 (A–D) or after rest in culture ex vivo, presumably without the self-stimulation (E). Online supplemental material is available at <http://www.jem.org/cgi/content/full/jem.20080611/DC1>.

We would like to thank Leni Abraham and Matt Jared for technical assistance in the preparation of recombinant monoclonal antibodies. Also, we thank Arlene Wilson, Zena Peters, and the Oklahoma Blood Institute for providing the blood. In addition, we acknowledge Sheryl Christofferson and the Oklahoma Medical Research Foundation sequencing core for all DNA sequencing, and Jacob Bass, Diana Hamilton, and the Oklahoma Medical Research Foundation flow core for all flow cytometry. Dr. J. Donald Capra, Judith James, and Dr. Mark Coggeshall were instrumental in reviewing the manuscript and for extensive discussion. Dr. Inaqui Sanz provided helpful suggestions.

This work was funded by National Institutes of Health grant P20RR018758-01 (P.C. Wilson).

The authors have no conflicting financial interests.

Submitted: 21 March 2008

Accepted: 2 December 2008

## REFERENCES

- Wardemann, H., S. Yurasov, A. Schaefer, J.W. Young, E. Meffre, and M.C. Nussenzweig. 2003. Predominant autoantibody production by early human B cell precursors. *Science*. 301:1374–1377.
- Gay, D., T. Saunders, S. Camper, and M. Weigert. 1993. Receptor editing: an approach by autoreactive B cells to escape tolerance. *J. Exp. Med.* 177:999–1008.
- Tiegs, S.L., D.M. Russell, and D. Nemazee. 1993. Receptor editing in self-reactive bone marrow B cells. *J. Exp. Med.* 177:1009–1020.
- Talmage, D.W. 1957. Allergy and immunology. *Annu. Rev. Med.* 8:239–256.
- Burnet, F.M. 1976. A modification of Jerne's theory of antibody production using the concept of clonal selection. *CA Cancer J. Clin.* 26:119–121.
- Nossal, G.J., and B.L. Pike. 1980. Clonal anergy: persistence in tolerant mice of antigen-binding B lymphocytes incapable of responding to antigen or mitogen. *Proc. Natl. Acad. Sci. USA*. 77:1602–1606.
- Nossal, G.J. 1983. Cellular mechanisms of immunologic tolerance. *Annu. Rev. Immunol.* 1:33–62.
- Goodnow, C.C. 1996. Balancing immunity and tolerance: deleting and tuning lymphocyte repertoires. *Proc. Natl. Acad. Sci. USA*. 93:2264–2271.
- Goodnow, C.C., J. Crosbie, S. Adelstein, T.B. Lavoie, S.J. Smith-Gill, R.A. Brink, H. Pritchard-Briscoe, J.S. Wotherspoon, R.H. Loblay, K. Raphael, et al. 1988. Altered immunoglobulin expression and functional silencing of self-reactive B lymphocytes in transgenic mice. *Nature*. 334:676–682.
- Goodnow, C.C., J. Crosbie, H. Jorgensen, R.A. Brink, and A. Basten. 1989. Induction of self-tolerance in mature peripheral B lymphocytes. *Nature*. 342:385–391.
- Cooke, M.P., A.W. Heath, K.M. Shokat, Y. Zeng, F.D. Finkelman, P.S. Linsley, M. Howard, and C.C. Goodnow. 1994. Immunoglobulin signal transduction guides the specificity of B cell–T cell interactions and is blocked in tolerant self-reactive B cells. *J. Exp. Med.* 179:425–438.
- Hartley, S.B., J. Crosbie, R. Brink, A.B. Kantor, A. Basten, and C.C. Goodnow. 1991. Elimination from peripheral lymphoid tissues of self-reactive B lymphocytes recognizing membrane-bound antigens. *Nature*. 353:765–769.
- Merrell, K.T., R.J. Benschop, S.B. Gauld, K. Aviszus, D. Decote-Ricardo, L.J. Wysocki, and J.C. Cambier. 2006. Identification of anergic B cells within a wild-type repertoire. *Immunity*. 25:953–962.
- Teague, B.N., Y. Pan, P.A. Mudd, B. Nakken, Q. Zhang, P. Szodoray, X. Kim-Howard, P.C. Wilson, and A.D. Farris. 2007. Cutting edge: Transitional T3 B cells do not give rise to mature B cells, have undergone selection, and are reduced in murine lupus. *J. Immunol.* 178:7511–7515.
- Cambier, J.C., S.B. Gauld, K.T. Merrell, and B.J. Vilen. 2007. B-cell anergy: from transgenic models to naturally occurring anergic B cells? *Nat. Rev. Immunol.* 7:633–643.
- Acevedo-Suarez, C.A., C. Hulbert, E.J. Woodward, and J.W. Thomas. 2005. Uncoupling of anergy from developmental arrest in anti-insulin B cells supports the development of autoimmune diabetes. *J. Immunol.* 174:827–833.
- Rojas, M., C. Hulbert, and J.W. Thomas. 2001. Anergy and not clonal ignorance determines the fate of B cells that recognize a physiological autoantigen. *J. Immunol.* 166:3194–3200.
- Erikson, J., M.Z. Radic, S.A. Camper, R.R. Hardy, C. Carmack, and M. Weigert. 1991. Expression of anti-DNA immunoglobulin transgenes in non-autoimmune mice. *Nature*. 349:331–334.
- Roark, J.H., A. Bui, K.A. Nguyen, L. Mandik, and J. Erikson. 1997. Persistence of functionally compromised anti-double-stranded DNA B cells in the periphery of non-autoimmune mice. *Int. Immunol.* 9:1615–1626.
- Nguyen, K.A., L. Mandik, A. Bui, J. Kavalier, A. Norvell, J.G. Monroe, J.H. Roark, and J. Erikson. 1997. Characterization of anti-single-stranded DNA B cells in a non-autoimmune background. *J. Immunol.* 159:2633–2644.
- Benschop, R.J., K. Aviszus, X. Zhang, T. Manser, J.C. Cambier, and L.J. Wysocki. 2001. Activation and anergy in bone marrow B cells of a novel immunoglobulin transgenic mouse that is both hapten specific and autoreactive. *Immunity*. 14:33–43.
- Borrero, M., and S.H. Clarke. 2002. Low-affinity anti-Smith antigen B cells are regulated by anergy as opposed to developmental arrest or differentiation to B-1. *J. Immunol.* 168:13–21.
- Pugh-Bernard, A.E., G.J. Silverman, A.J. Cappione, M.E. Villano, D.H. Ryan, R.A. Insel, and I. Sanz. 2001. Regulation of inherently autoreactive VH4-34 B cells in the maintenance of human B cell tolerance. *J. Clin. Invest.* 108:1061–1070.
- Zheng, N.Y., K. Wilson, X. Wang, A. Boston, G. Kolar, S.M. Jackson, Y.J. Liu, V. Pascual, J.D. Capra, and P.C. Wilson. 2004. Human immunoglobulin selection associated with class switch and possible tolerogenic origins for C delta class-switched B cells. *J. Clin. Invest.* 113:1188–1201.
- Koelsch, K., N.Y. Zheng, Q. Zhang, A. Duty, C. Helms, M.D. Mathias, M. Jared, K. Smith, J.D. Capra, and P.C. Wilson. 2007. Mature B cells class switched to IgD are autoreactive in healthy individuals. *J. Clin. Invest.* 117:1558–1565.
- Cappione, A. III, J.H. Anolik, A. Pugh-Bernard, J. Barnard, P. Dutcher, G. Silverman, and I. Sanz. 2005. Germinal center exclusion of autoreactive B cells is defective in human systemic lupus erythematosus. *J. Clin. Invest.* 115:3205–3216.
- Wrammert, J., K. Smith, J. Miller, T. Langley, K. Kokko, C. Larsen, N.Y. Zheng, I. Mays, C. Helms, J. James, et al. 2008. Rapid cloning of high affinity human monoclonal antibodies against influenza virus. *Nature*. 453:667–671.
- Koffler, D., R.I. Carr, V. Agnello, T. Fiezi, and H.G. Kunkel. 1969. Antibodies to polynucleotides: distribution in human serums. *Science*. 166:1648–1649.
- Stollar, B.D., G. Zon, and R.W. Pastor. 1986. A recognition site on synthetic helical oligonucleotides for monoclonal anti-native DNA autoantibody. *Proc. Natl. Acad. Sci. USA*. 83:4469–4473.
- Radic, M.Z., and M. Weigert. 1995. Origins of anti-DNA antibodies and their implications for B-cell tolerance. *Ann. N. Y. Acad. Sci.* 764:384–396.
- Bradwell, A.R., R.P. Stokes, and G.D. Johnson. 1995. Atlas of HEp-2 patterns. The Binding Site LTD, Birmingham, England. 118 pp.
- Sims, G.P., R. Ettinger, Y. Shirota, C.H. Yarboro, G.G. Illei, and P.E. Lipsky. 2005. Identification and characterization of circulating human transitional B cells. *Blood*. 105:4390–4398.
- Tedder, T.F., J. Tuscano, S. Sato, and J.H. Kehrl. 1997. CD22, a B lymphocyte-specific adhesion molecule that regulates antigen receptor signaling. *Annu. Rev. Immunol.* 15:481–504.



34. Wirths, S., and A. Lanzavecchia. 2005. ABCB1 transporter discriminates human resting naive B cells from cycling transitional and memory B cells. *Eur. J. Immunol.* 35:3433–3441.
35. Meffre, E., E. Davis, C. Schiff, C. Cunningham-Rundles, L.B. Ivashkiv, L.M. Staudt, J.W. Young, and M.C. Nussenzweig. 2000. Circulating human B cells that express surrogate light chains and edited receptors. *Nat. Immunol.* 1:207–213.
36. Meffre, E., A. Schaefer, H. Wardemann, P. Wilson, E. Davis, and M.C. Nussenzweig. 2004. Surrogate light chain expressing human peripheral B cells produce self-reactive antibodies. *J. Exp. Med.* 199:145–150.
37. Carsetti, R., M.M. Rosado, and H. Wardmann. 2004. Peripheral development of B cells in mouse and man. *Immunol. Rev.* 197:179–191.
38. Bikah, G., J. Carey, J.R. Ciallella, A. Tarakhovsky, and S. Bondada. 1996. CD5-mediated negative regulation of antigen receptor-induced growth signals in B-1 B cells. *Science*. 274:1906–1909.
39. Miller, R.A., and J. Gralow. 1984. The induction of Leu-1 antigen expression in human malignant and normal B cells by phorbol myristate acetate (PMA). *J. Immunol.* 133:3408–3414.
40. Wilson, P.C., O. de Bouteiller, Y.J. Liu, K. Potter, J. Banchereau, J.D. Capra, and V. Pascual. 1998. Somatic hypermutation introduces insertions and deletions into immunoglobulin V genes. *J. Exp. Med.* 187:59–70.
41. Wilson, P.C., K. Wilson, Y.J. Liu, J. Banchereau, V. Pascual, and J.D. Capra. 2000. Receptor revision of immunoglobulin heavy chain variable region genes in normal human B lymphocytes. *J. Exp. Med.* 191:1881–1894.
42. Zheng, N.Y., K. Wilson, M. Jared, and P.C. Wilson. 2005. Intricate targeting of immunoglobulin somatic hypermutation maximizes the efficiency of affinity maturation. *J. Exp. Med.* 201:1467–1478.
43. Liu, Y.J., O. de Bouteiller, C. Arpin, F. Briere, L. Galibert, S. Ho, H. Martinez-Valdez, J. Banchereau, and S. Lebecque. 1996. Normal human IgD+IgM- germinal center B cells can express up to 80 mutations in the variable region of their IgD transcripts. *Immunity*. 4:603–613.
44. Arpin, C., O. de Bouteiller, D. Razanajaona, I. Fugier-Vivier, F. Briere, J. Banchereau, S. Lebecque, and Y.J. Liu. 1998. The normal counterpart of IgD myeloma cells in germinal center displays extensively mutated IgVH gene, C $\mu$ -C $\delta$  switch, and  $\lambda$  light chain expression. *J. Exp. Med.* 187:1169–1178.
45. Ichiyoshi, Y., and P. Casali. 1994. Analysis of the structural correlates for antibody polyreactivity by multiple reassortments of chimeric human immunoglobulin heavy and light chain V segments. *J. Exp. Med.* 180:885–895.
46. Klonowski, K.D., L.L. Primiano, and M. Monestier. 1999. Atypical VH-D-JH rearrangements in newborn autoimmune MRL mice. *J. Immunol.* 162:1566–1572.
47. Link, J.M., and H.W.J. Schroeder. 2002. Clues to the etiology of autoimmune diseases through analysis of immunoglobulin genes. *Arthritis Res.* 4:80–83.
48. Healy, J.I., R.E. Dolmetsch, L.A. Timmerman, J.G. Cyster, M.L. Thomas, G.R. Crabtree, R.S. Lewis, and C.C. Goodnow. 1997. Different nuclear signals are activated by the B cell receptor during positive versus negative signaling. *Immunity*. 6:419–428.
49. Dolmetsch, R.E., R.S. Lewis, C.C. Goodnow, and J.I. Healy. 1997. Differential activation of transcription factors induced by Ca<sup>2+</sup> response amplitude and duration. *Nature*. 386:855–858.
50. Vilen, B.J., K.M. Burke, M. Sleater, and J.C. Cambier. 2002. Transmodulation of BCR signaling by transduction-incompetent antigen receptors: implications for impaired signaling in anergic B cells. *J. Immunol.* 168:4344–4351.
51. Weintraub, B.C., J.E. Jun, A.C. Bishop, K.M. Shokat, M.L. Thomas, and C.C. Goodnow. 2000. Entry of B cell receptor into signaling domains is inhibited in tolerant B cells. *J. Exp. Med.* 191:1443–1448.
52. Gauld, S.B., R.J. Benschop, K.T. Merrell, and J.C. Cambier. 2005. Maintenance of B cell anergy requires constant antigen receptor occupancy and signaling. *Nat. Immunol.* 6:1160–1167.
53. Raff, M.C., J.J. Owen, M.D. Cooper, A.R. Lawton III, M. Megson, and W.E. Gathings. 1975. Differences in susceptibility of mature and immature mouse B lymphocytes to anti-immunoglobulin-induced immunoglobulin suppression in vitro. Possible implications for B-cell tolerance to self. *J. Exp. Med.* 142:1052–1064.
54. Goodnow, C.C., R. Brink, and E. Adams. 1991. Breakdown of self-tolerance in anergic B lymphocytes. *Nature*. 352:532–536.
55. Eris, J.M., A. Basten, R. Brink, K. Doherty, M.R. Kehry, and P.D. Hodgkin. 1994. Anergic self-reactive B cells present self antigen and respond normally to CD40-dependent T-cell signals but are defective in antigen-receptor-mediated functions. *Proc. Natl. Acad. Sci. USA*. 91:4392–4396.
56. Chang, N.H., T. McKenzie, G. Bonventi, C. Landolt-Marticorena, P.R. Fortin, D. Gladman, M. Urowitz, and J.E. Wither. 2008. Expanded population of activated antigen-engaged cells within the naive B cell compartment of patients with Systemic Lupus Erythematosus. *J. Immunol.* 180:1276–1284.
57. Pascual, V., Y.J. Liu, A. Magalski, O. de Bouteiller, J. Banchereau, and J.D. Capra. 1994. Analysis of somatic mutation in five B cell subsets of human tonsil. *J. Exp. Med.* 180:329–339.